



Full length article



## A comparative approach employing microCT for the analysis of Cenozoic foraminifera from the Brazilian carbonate equatorial platform

Olga Oliveira De Araújo<sup>a</sup>, Orangel Aguilera<sup>b,\*</sup>, Dayana Alvarado Sierra<sup>c</sup>,  
 Beatriz Teixeira Guimarães<sup>c</sup>, Vinicius Kutter<sup>c</sup>, Ana Paula Linhares<sup>d</sup>, Daniel Lima<sup>e</sup>,  
 Julianny Dos Santos Silva<sup>b</sup>, Ricardo Tadeu Lopes<sup>a</sup>

<sup>a</sup> Federal University of Rio de Janeiro (UFRJ), Nuclear Instrumentation Laboratory, Nuclear Engineering Program/COPPE, Av. Horácio Macedo, Cidade Universitária, Rio de Janeiro, 21941-450, Brazil

<sup>b</sup> Fluminense Federal University (UFF), Rua Prof. Marcos Waldemar de Freitas Reis, Paleocology and Global Changes Laboratory, Campus Gragoatá, Bloco M, Lab 110, Niterói, Rio de Janeiro, 24210-201, Brazil

<sup>c</sup> Federal University of Pará (UFPA), Geoscience Institute, Belém, Pará, 66075-110, Brazil

<sup>d</sup> Museu Paraense Emílio Goeldi, Earth Sciences and Ecology Coordination, Belém, Pará, 66077-830, Brazil

<sup>e</sup> Museu de Paleontologia Plácido Cidade Nuvens, Universidade Regional do Cariri (URCA), Santana do Cariri, Ceará, 63190-000, Brazil

### ARTICLE INFO

**Keywords:**  
 Micropaleontology  
 MicroCT  
 Petrography  
 Foraminifera 3D database

### ABSTRACT

Worldwide, some of the largest hydrocarbon reservoirs are located in tropical neritic carbonate deposits. Biostratigraphic and paleoenvironmental analyzes of these sedimentary records are often based on the study of foraminiferal assemblage. Foraminifera-based biozones are widely employed in the oil industry to support drilling processes that, alongside petrophysical prospecting, define interval favorable for exploiting hydrocarbon resources. Both scientific research and the petroleum industry, however, usually apply traditional petrographical and paleontological methods to analyze microfossil assemblages, especially for large benthic foraminifera. New, faster, and more accurate methods based on microCT analyzes have emerged as a valuable high-output tool to obtain high-resolution microfossil records for biostratigraphy and paleoenvironmental reconstructions. This method is also useful for the development of digital databases for artificial intelligence applications. MicroCT analyzes, therefore, lead to faster identification of foraminifera assemblage and support digital access to international foraminifera repositories and reference collections, introducing a new dimension in micropaleontological research.

### 1. Introduction

Some of the most important hydrocarbon reservoirs in the world are located within carbonate deposits (Khodja et al., 2020). Tropical carbonate platform successions, in particular, contain some of the largest known reservoirs, such as the Arab-D Formation in Saudi Arabia (Pemberton and Gingras, 2005; Al-Awwad and Collins, 2013), the Asmari Formation in Iran (Perry and Choquette, 1985; Amirshankarami et al., 2007; Coletti et al., 2017; Mahmoodabadi and Zahiri, 2022), the Perla limestone in Venezuela (Castillo et al., 2017; Coletti et al., 2017), the French Guiana-Guyana-Suriname plays (Wong and Geuns, 2019), and some of the Pre-salt fields at the Campos Basin in Brazil (Bruhn et al., 2003).

Off-shore, Paleocene to Miocene, neritic carbonate deposits of the

Brazilian equatorial platform are often characterized by a remarkable abundance of large benthic foraminifera (LBF) (Abreu et al., 1986; de Mello e Sousa, 1994; Pessoa-Neto, 1999; de Mello e Sousa et al., 2003; BouDagher-Fadel and Price, 2010a, 2010b; BouDagher-Fadel et al., 2010; Alvarado et al., 2023). The Miocene of the Brazilian equatorial platform, outcropping along the coastal plain is characterized by the occurrence of small and large benthic foraminifera and planktonic foraminifera (Petri, 1954, 1957; Távora and Fernandes, 1999; Rojas et al., 2022; Teixeira et al., 2024). Foraminiferal assemblages are useful in identifying biozones and determining or constraining ages within these deposits.

Until now, the academy and the oil industry have routinely applied traditional geological methods to obtain petrographic thin sections from cores for microfossil analyzes. These can be also used by

\* Corresponding author.

E-mail address: [orangelaguilera@id.uff.br](mailto:orangelaguilera@id.uff.br) (O. Aguilera).

<https://doi.org/10.1016/j.micron.2024.103611>

Received 20 October 2023; Received in revised form 9 February 2024; Accepted 13 February 2024

Available online 15 February 2024

0968-4328/© 2024 Elsevier Ltd. All rights reserved.

biostratigraphers to analyze the morphological parameters of embryonic structures which are in turn fundamental in the identification of LBF species (e.g., [Muhammed and Ghafor, 2008](#); [Ghafor, 2014](#); [Benedetti et al., 2017](#); [Torres-Silva et al., 2017](#); [Coletti et al., 2018](#); [Cotton et al., 2018](#); [Hohenegger and Torres-Silva, 2020](#)). Although disaggregation of lithified carbonate rocks, employing mechanical, chemical, or physical methods may still be the best way to recover isolated and well-preserved foraminifera samples ([Malik et al., 2022](#)), and although wet sieving (2 mm, 500  $\mu\text{m}$ , 250  $\mu\text{m}$ , 125  $\mu\text{m}$ , and 65  $\mu\text{m}$  meshes) is still the most advantageous method to recover microfossils from non-lithified rocks ([Green, 2001](#)), fast and accurate methods based on microCT imaging are currently been developed.

The microCT imaging method allows obtaining high-resolution details of the inner and outer morphology of LBF, which are useful for species identification ([Görög et al., 2011](#); [Ferrández-Cañadell et al., 2014](#); [Aguilera et al., 2020a, 2020b](#); [Mouro et al., 2021](#); [François et al., 2022](#); [Alvarado et al., 2023](#)). This approach can allow detailed analyses of the internal structures (e.g., [Briguglio et al., 2014, 2016](#)), but it can also be used to acquire large amounts of data in a much shorter time frame in comparison to classical paleontological and petrographical approaches (e.g., [Coletti et al., 2018](#)).

3D analyzes and reconstruction of foraminifera could be used to create digital repositories and provide data that could be used in machine learning, leading to the development of fossil guides for taxonomic and biostratigraphic applications.

Thus, the present study aims to compare different methods of analyzing foraminifera assemblages (stereomicroscope, petrographic microscope, scanning electronic microscope, and computer digital tomography) using core cutting and lithified rock samples, in order to precisely recognize the most accurate, time- and cost-effective procedure.

## 2. Geological setting

The Ilha de Santana Formation ([Brandão and Feijó, 1994](#); [Figueiredo et al., 2007](#); [Soares et al., 2007](#)) is situated within the Humberto de Campos Group in the Pará-Maranhão and the Barreirinhas basins of the Brazilian equatorial platform ([Fig. 1](#)). This formation comprises an extensive carbonate package from the Cretaceous (Maastrichtian) and encompasses a substantial portion of the Cenozoic (Oligocene and Miocene), consisting of i) calcarenites and calcirudites, deposited in the inner platform; ii) calcarenites and calcilitites, deposited in the middle platform; and iii) marls, shales, and mudstones, deposited in the outer platform and along the slope ([Brandão and Feijó, 1994](#); [Figueiredo et al., 2007](#)). The section of 1-MAS-16-MA (between 798 and 1200 m below the sea surface (mbsf) from the Ilha de Santana Formation, the object of this study, has an age spanning from Chattian to Burdigalian ([Alvarado et al., 2023](#)). This interval represents the initial biofacies BF-6 to initial biofacies BF-3 of the Ilha de Santana Formation, dominated by fragments of calcareous algae and LBF ([Alvarado et al., 2023](#)).

The Pirabas Formation ([Maury, 1925](#)) is well-recognized through equatorial coastal plain outcrops and quarries located in the Pará state, Brazil ([Fig. 1](#)). It is characterized by a mixture of carbonatic-siliciclastic deposits formed in shallow water context ranging from the inner to the middle platform ([Rossetti et al., 2013](#); [Aguilera et al., 2020a, 2020b, 2022](#)), spanning from the late early Miocene to the late middle Miocene. However, recent studies examining from the Ilha de Fortaleza in the Ponta do Castelo and the Fazenda outcrops suggest an age of late early Miocene (Burdigalian) ([Gomes et al., 2023](#)). It is deposited over Precambrian rocks and it is overlain by the siliciclastic deposits of the Barreiras Formation ([Rossetti et al., 1989](#); [Rossetti, 2006](#)). [Aguilera et al. \(2022\)](#) distinguish four main facies within the Pirabas Formation: i) facies  $\alpha_1$ , shallow-water offshore platform characterized by

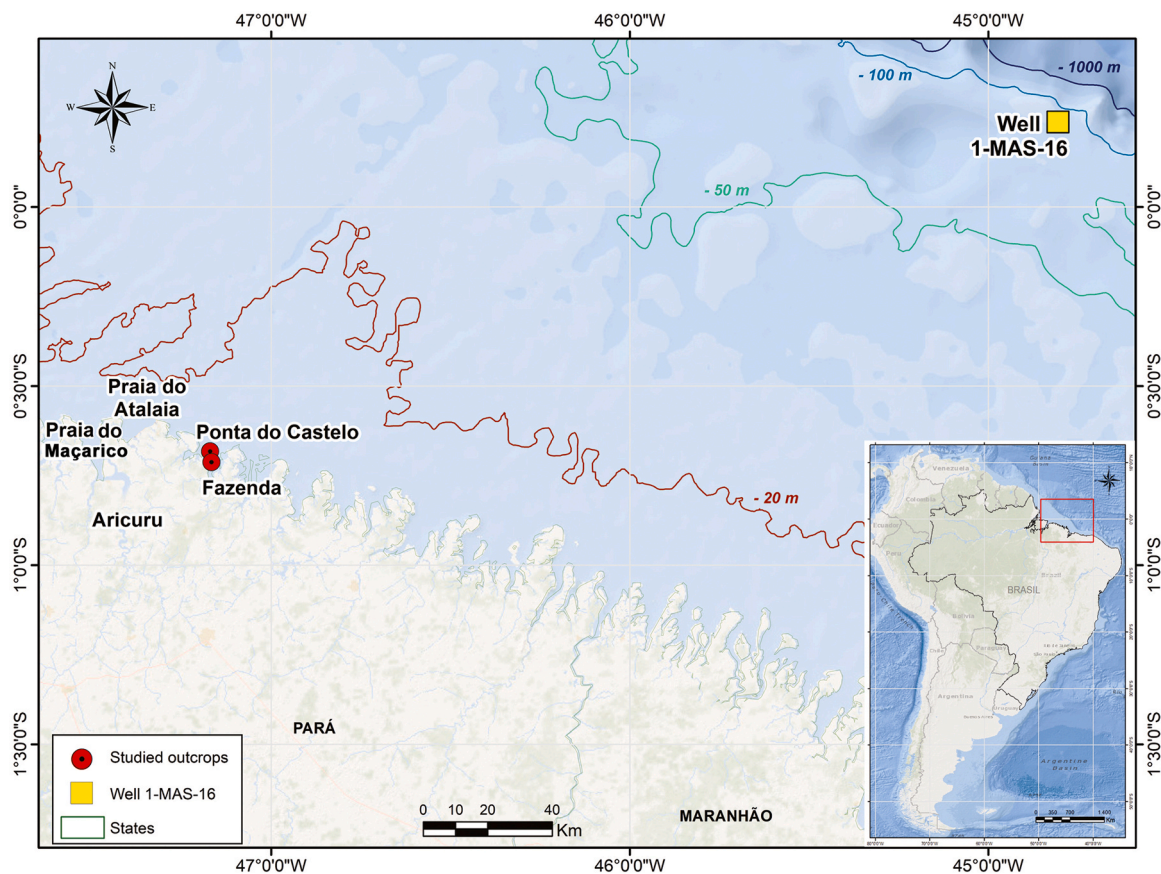


**Fig. 1.** Map indicating the well 1-MAS-16-MA location within the Pará-Maranhão Basin, Ilha de Santana Formation (yellow square) and the carbonate outcrops of Pirabas Formation (red dots) at the Pará state coast, Brazil.

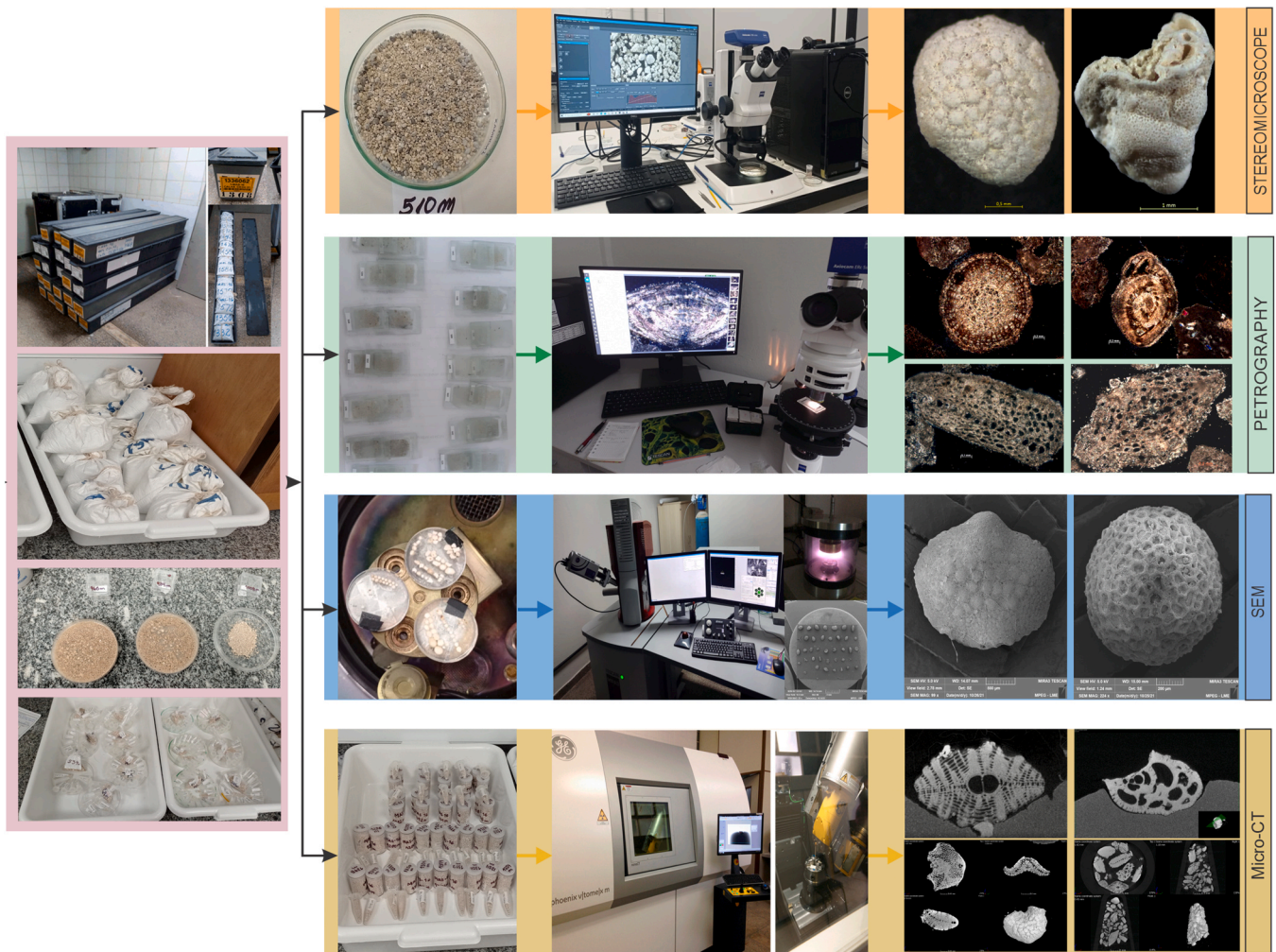


**Fig. 2.** Simplified diagram of the methodology applied herein to the micropaleontology analysis of cutting samples from the Ilha de Santana Formation (well 1-MAS-16-MA), Pará-Maranhão Basin, Brazil. Sub-sample treatment, microfossil picking, and digital recording by stereomicroscopy, petrography microscopy, scanning electron microscopy, and computer scanner microtomography. Note the digital specimen images and structures details.

echinoderm-bryozoan packstone to rudstone (with  $\leq 10\%$  of siliciclastic content in the rock); ii) facies  $\alpha_2$ , shallow-water inner platform, comprising siliciclastic-rich wackestone to packstone (with siliciclastic content ranging between 10% and 30%); iii) facies  $\beta$ , shallow coastal plain dominated by siliciclastic fine-grained sandstone to mudstone (with  $\geq 50\%$  siliciclastic content); and, iv) facies  $\gamma$ , restricted tidal coastal plain of marginal mangroves dominated by sand-sized angular grains, iron-rich nodules, and pyritized fossils. The lithified rock samples studied here come from the Ilha de Fortaleza (Ponta do Castelo and Fazenda outcrops) represent the facies  $\alpha_1$ .

### 3. Material and methods

#### 3.1. Cuttings

Ten cutting samples from the 798–1200 mbsf section of the well 1-MAS-16-MA (Chattian to Burdigalian) were analyzed. These samples were loaned by the Brazilian National Petroleum Agency (ANP, Protocol SAA 46.19) for this study. A schematic diagram of the sampling analysis methods employed herein is depicted in Fig. 2.

Cutting samples from this section are characterized by the presence of LBF e.g., miogypsinids and lepidocyclinids. Therefore, the study of inner diagnostic structures is mandatory in order to correctly identify the different taxa.

Step 1 (pretreatment and stereomicroscopy). Cutting samples from the core were quartered and separated into  $12\text{ mm}^3$  sub-samples. Each sub-sample was placed on a glass Petri dish, treated with 4% acetic acid for three minutes, washed under running water, sieved through a  $125\text{ }\mu\text{m}$  mesh, and dried at  $28^\circ\text{C}$ . The LBF present in the samples were observed with a stereomicroscope, separated, picked, counted, and placed into sterile polypropylene Eppendorf vials using fine brushes.

Step 2 (metallization and scanning electron microscopy). LBF specimens were selected for detailed external morphology assessments by scanning electron microscopy (SEM). The specimens were attached to 12 mm-diameter aluminum supports using double-sided carbon adhesive tape and metallized with Au for 90 s. Metallization resulted in a thin gold film, averaging 12 nm in thickness, over the sample surface. Images were generated using a secondary electron detector and applying a voltage acceleration between 5 and 1 kV and a working distance of about 15 mm.

Step 3 (microcomputer tomography). MicroCT scan acquisitions and 3D digital imaging of sorted LBF (specimens) were performed on cutting sub-samples stored in a 1.5 mL sterile polypropylene Eppendorf using a microcomputer tomograph v|tome|x M 300 with an X-ray microfocus CT system (BHGE). Scanning parameters were set at 60 kV voltage,  $100\text{ }\mu\text{A}$  current, 333 ms exposure time per scan, 1 mm-thick Al filter,  $6\text{ }\mu\text{m}$  voxel size resolution and a total of 1500 scans within a  $360^\circ$  rotation. The Phoenix Data X Reconstruction v. 2.2 (GE) software was used for the 3D

reconstructions, employing slice alignment, beam hardening correction, and ring artifact reduction. A mathematical edge-enhancement filter was applied to achieve higher LBF contrast. The VG Studio Max v 3.0 and Avizo v. 2021.1 software were used for 3D visualizations and the plates were edited using Photoshop 2020.

Step 4 (virtual analyzes, measurements, and identification). The biometric LBF analyzes were based on equatorial section measurements of individual foraminiferal tests following the standard methods used in the identification of LBF species (Van der Vlerk, 1959, 1963; Matteucci and Schiavinotto, 1977; Van Vessem, 1978; Schiavinotto, 1978; Chaproniere, 1980; Muhammed and Ghafor, 2008; Less et al., 2008; Özcan et al., 2009; Ghafor, 2014; Renema and Cotton, 2015; Benedetti et al., 2017; Torres-Silva et al., 2017; Coletti, et al., 2018; Hohenegger and Torres-Silva, 2020). Taxonomic identifications follow in particular the main references for Cenozoic LBF assemblages (Robinson, 2003; de Mello e Sousa et al., 2003, 2009; Fiorini and Jaramillo, 2007; Brandano et al., 2009; BouDagher-Fadel and Price, 2010a, b; BouDagher-Fadel et al., 2010; Albert-Villanueva et al., 2017; BouDagher-Fadel, 2018; Coletti et al., 2018; Özcan et al., 2019; Mitchell et al., 2022).

Step 5 (petrographic thin sections). Cutting sub-samples of around 3g each were placed in a plastic form, embedded in an acrylic resin block, cut, fixed on 76 ×26 mm glass slides, and polished to 30 µm thickness. A total of 31 petrographical thin sections were then

qualitatively and quantitatively analyzed for foraminifera assessments. Photomicrographs were obtained using a petrographic microscope equipped with an integrated digital system.

Step 6 (microcomputer tomography, virtual analyzes, and identification). A total of 10 unsorted bulks of cutting sub-samples (not only with LBF but including also all the bioclasts, skeletal grains, and aggregates constituting the cutting sub-samples) were placed into 1.5 mL sterile polypropylene Eppendorf vials and analyzed by microCT acquisition, processed using the AVIZO software to capture digital coronal, sagittal and axial planes (six thousand sections) and sequentially edited using the Windows Media Video software (WMV format) to identify and determine LBF assemblage.

### 3.2. Lithified carbonate rock

A total of 13 lithified carbonate rock samples from the Pirabas Formation (Burdigalian) were collected in the type locality of the Ilha de Fortaleza (Ponta do Castelo and Fazenda outcrops) along the coastal marine platform of Pará state (Aguilera et al., 2022, 2023). A schematic diagram is depicted in Fig. 3.

Disaggregated samples from lithified rocks are characterized by the absence of LBF in these outcrop sections e.g., miogypsinids and lepidocyclinids. In this sense, most of the identification of the small benthic



Fig. 3. Simplified diagram of the methodology applied herein to the micropaleontology analysis of lithified rocks samples from the Pirabas Formation (Ponta do Castelo and Fazenda outcrops), Pará state, Brazil. Sub-sample treatment for rock disaggregation, microfossil picking, and digital recording employing stereo-microscopy, petrography microscopy, scanning electron microscopy, and computer scanner microtomography. Note the digital specimen images, structure details, and digital plug sub-sample.

**Table 1**

Foraminifera. Species abundance per method (picking, petrography, and microCT) from the Ilha de Santana Formation (Oligocene/Miocene section), 1-MAS-16-MA well, Pará-Maranhão Basin, Brazilian equatorial platform.

FORAMINIFERA (species/specimens number per methods)													FORAMINIFERA (dominant species per methods in %)					Counts (n) and relative proportion (%)									
Cuttings samples depth (m)	Methods *Picking (12 mm3), *Petrography (2), *MicroCT (coronal & axial)	Amphistegina	Migypsina	Lepidocyclina	Eulepidina	Victoriella	Heterostegina	Sphaerogypsina	Planorbulinella	Nummulites	Archaia	Sorites	Textularia	Pyrgo	Operculina	SBHyaline	SBP-orcaneous	Cuttings samples depth (m)	Methods *Picking (12 mm3), *Petrography (2), *MicroCT (coronal & axial)	Amphistegina	Migypsina	Lepidocyclina	Victoriella	Heterostegina	counts all species by method	proportion all species by method	
798	Picking	250	203	50	2	1	2												Picking	56.3	40.0	50.5	16.7		509	47.0	
	Petrography	45	26	7															Petrography	10.1	5.2	7.1			78	7.2	
	MicroCT	149	278	42	10					1			1	1	1				MicroCT	33.6	54.8	42.4	83.3		496	45.8	
804	Picking	836	488	237	3	1	11												Picking	86.1	52.7	53.9	9.7		1576	65.7	
	Petrography	38	65	15	1						1								Petrography	3.9	7.0	3.4	3.2		120	5.0	
	MicroCT	97	373	188	27				1	2						1	3	12	MicroCT	10	40.3	42.3	87.1		704	29.3	
846	Picking	49	142	128	5	2	2												Picking	62.0	40.7	56.6	6.0		328	43.4	
	Petrography	3	4	8	1														Petrography	3.8	1.1	3.5	1.2		16	2.1	
	MicroCT	27	203	90	78													9	5	MicroCT	34.2	58.2	39.8	92.9		412	54.5
858	Picking	69	129	156	4	2													Picking	32.1	29.5	37.9	5.4		360	30.8	
	Petrography	4	5	15	7														Petrography	1.8	1.1	3.6	9.5		31	2.65	
	MicroCT	142	304	242	63			3			1							23	MicroCT	66.0	69.4	58.6	85.1		778	66.55	
1008	Picking	2	97	36	1	141	1	4											Picking	9.1	28.8	26.5	0.8	33.7	282	25.0	
	Petrography	5	7	25	2	24							1	1					Petrography	22.7	2.1	18.4	1.5	5.7	66	5.8	
	MicroCT	15	233	75	131	254			1		1				6	7	58		MicroCT	68.2	69.1	55.1	97.8	60.6	781	69.2	
1020	Picking	2	96	54	1	113													Picking	14.3	32.7	43.5	0.4	32.8	266	25.3	
	Petrography	4	7	9	3														Petrography	28.6	2.4	7.3	0.9		23	2.2	
	MicroCT	8	191	61	228	228		2										11	32	MicroCT	57.1	65.0	49.2	99.6	66.3	761	72.5
1032	Picking	1	22	16		37													Picking	7.1	14.1	20.5	18.4		76	10.54	
	Petrography	1	8	8		4													Petrography	7.1	5.1	10.3	2.0		21	2.91	
	MicroCT	12	126	54	90	160		1	21									10	37	113	MicroCT	85.7	80.8	69.2	100	79.6	624
1074	Picking	17	23	105	3	122	2												Picking	51.5	41.1	70.5	5.9	46.0	272	38.15	
	Petrography	7	11	16		14													Petrography	21.2	19.6	10.7	5.2		48	6.73	
	MicroCT	9	22	28	48	129		33							4	9	111		MicroCT	27.2	39.3	18.8	94.1	48.7	393	55.12	
1164	Picking	6	3	26		80													Picking	37.5	60	14.5	60.6		115	19.23	
	Petrography	4		6		2													Petrography	25.0		3.4	1.5		12	2.01	
	MicroCT	6	2	147	8	50		165							25	10	58		MicroCT	37.5	40	82.1	100	37.9	471	78.76	
1200	Picking	3	20	3	28	1													Picking	15.8	11.3	1.8	80		55	10.44	
	Petrography	10	19	3	3			2							1	3			Petrography	52.6	10.7	1.8	8.6		41	7.78	
	MicroCT	6	138	1	164	4		66			1			3	14	34			MicroCT	31.6	78.0	96.5	11.4		431	81.78	
Foraminifera recovery (proportion in %) by method		Picking	Mean: 31.57		Petrography	Mean: 4.45		MicroCT	Mean: 63.98																		

and planktonic foraminifera assemblage is not fixed to the study of the inner diagnostic character.

Step 1 (pretreatment). A consolidated packstone from the Ponta do Castelo and the Fazenda outcrops located at Ilha de Fortaleza was disintegrated using around 1 kg of each sample. The rock fractions (1 kg each) were then immersed in common water within a beaker (without added soda or some other chemicals), and put over a heating plate at 70 °C for 72 h, replenishing the evaporated water when necessary. The disaggregated sediments were then washed and sieved through 500 µm, 250 µm, 180 µm, 125 µm, and 65 µm meshes and dried in an oven at 60°C for 48 h. 15 g of sample was separated for foraminifera picking using a splitter.

Step 2 (stereomicroscopy). Microfossils were separated, identified, counted, and photographed under a stereomicroscope coupled to a digital system.

Step 3 (microcomputer tomography and virtual analyzes). MicroCT scan and 3D reconstructions of the foraminifera were performed, following the previously described protocol, on non-disaggregated fragment of lithified packstone.

Step 4 (petrographic thin sections). A total of 31 petrographical thin sections were prepared using fragments of rocks with about 3 cm<sup>3</sup> of volume, following the standard method for thin sections preparation. The microphotographs were taken using a digital system coupled to a petrographic microscope.

### 3.3. Statistical analyzes

Relative abundances of foraminifera are calculated as the ratio between the number of specimens of a species (n) and the total number of specimens of all species in the same sample (T):  $RF = (n \times 100)/T$ . The relative frequencies are expressed as percentages. Absolute abundances expresses the number of times a taxon was recorded at each depth in the different analyzed methods. Similarity between methods was assessed using the Jaccard and Bray-Curtis indexes. All analyzes were conducted using PAST software (4.0) and further edited in Adobe Illustrator when necessary.

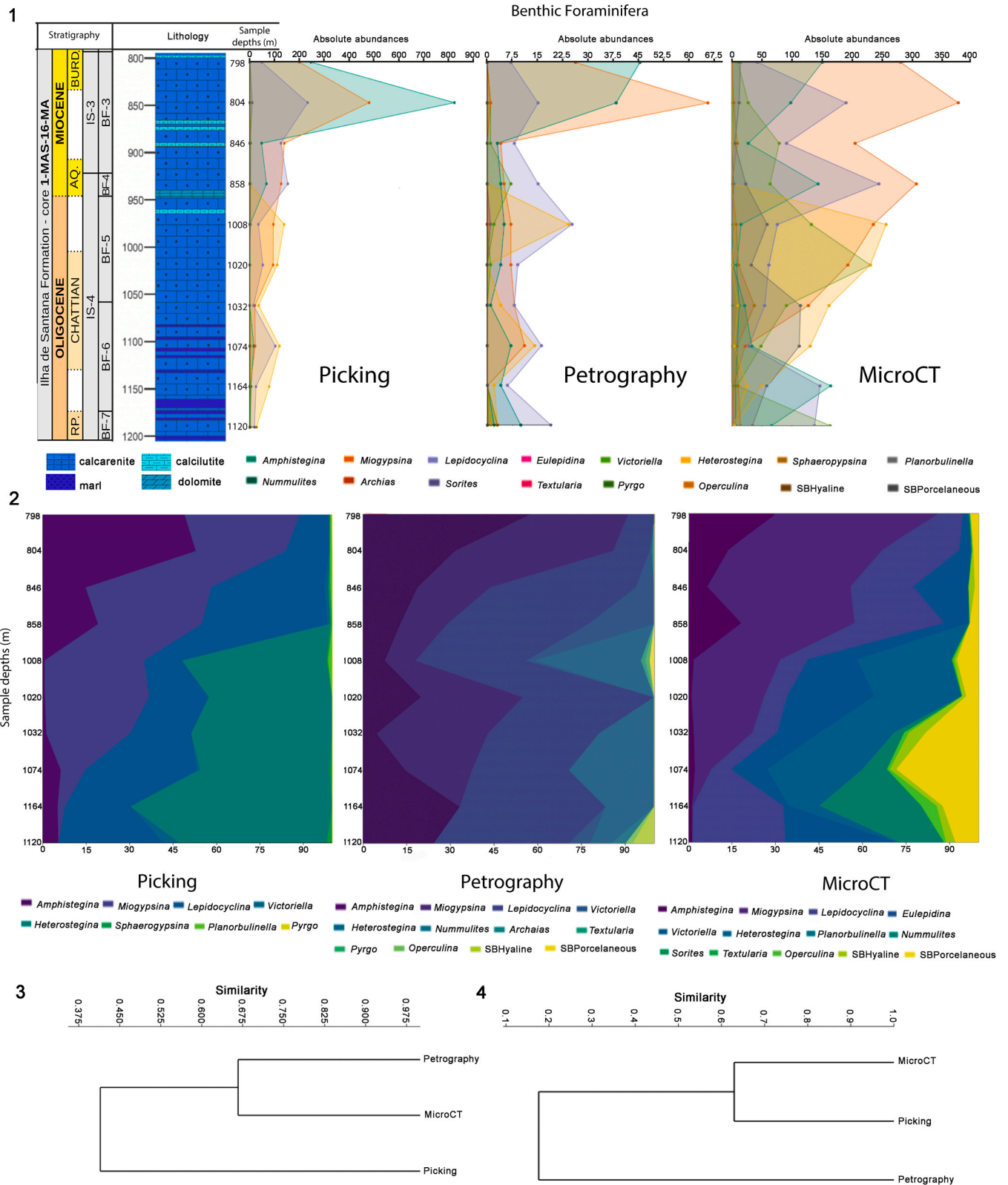


**Fig. 4.** Benthic foraminifera recovered from the Ilha de Santana Formation at well 1-MAS-16-MA using picking, petrography, and microCT methods. 1, absolute abundance. 2, relative abundance expressed as stacked areas. 3, clustering dendrogram based on taxa abundances (Bray-Curtis). 4, clustering dendrogram based on taxa occurrences (Jaccard). The geochronological time scale and lithology follows Alvarado et al. (2023).

4. Results

Table 1 and Figure 4.1 display the comparative cutting sample analyzes for foraminifera recovery, identification, and quantification. A total of 10,146 specimens were recovered in the cutting samples from well 1-MAS-16-MA, taking into account picking, petrography, and microCT methods. MicroCT was the most effective method for recovering benthic foraminifera (n= 5851), followed by picking (n= 3839) and petrography (n= 456). MicroCT also recovered the highest number of taxa (n= 13), followed by petrography (n= 12) and picking (n= 8) (Fig. 4.2).

The methods successfully recovered the index taxa (i.e., *Amphistegina*, *Miogyopsina*, *Lepidocyclina*, *Victoriella*, and *Heterostegina*); however, differences in absolute and relative frequencies were observed among the methods (Figs. 4.1, 4.2). *Amphistegina* was well-recovered in the picking method (n= 1235), whereas *Victoriella* was predominantly recovered by the microCT method (n= 847) and only minimally in the picking (n= 22) and petrography (n= 14) methods (Fig. 4.2).

MicroCT and petrography were the most effective methods for recovering the non-index taxa, with *Nummulites*, *Textularia*, *Operculina*, small benthic Hialine (SBHialine), and small benthic Porcelaneous (SBPorcelaneous) foraminifera exclusively recovered by these methods. *Eulepidina* and *Sorites* were exclusively recovered by the microCT method, while *Sphaerogypsina* and *Archaias* were exclusively recovered by picking and petrography, respectively (Fig. 4.2).

Considering the number of taxa recovered by all methods, microCT and petrography were the most similar, with 67% similarity (Fig. 4.3). On the other hand, when the abundances of taxa recovered are considered, microCT and picking showed about 65% similarity (Fig. 4.4).

Table 2 and Figs. 5 and 6 present results of the comparative lithified rock analyzes for foraminifera recovery, identification, and quantification. A total of 1693 specimens were recovered in the lithified rock

samples from the Pirabas Formation in the Ilha de Fortaleza outcrops, considering both picking and petrography. Picking was the most effective method for recovering benthic and planktonic foraminifera (n= 1449) followed by petrography (n= 244). Picking also recovered the highest number of taxa (n= 21), followed by petrography (n= 10) (Fig. 6). The methods successfully recovered the index taxa (i.e., *Amphistegina*, *Archaias*, *Cibicides*, *Discorbis*, *Pyrgo*, *Quinqueloculina*, and *Textularia*).

The microCT scans allowed for the visualization and measurement of inner LBF diagnostic structures (Fig. 7) necessary for accurate species identification and optimized working time (Table 3). The microCT method was able to explore digital frames in coronal, axial, and sagittal views and based on Table 1 (number of specimens) and 3 (time) improved the method for species/specimens sampling recovery compared to the petrographical thin sections and picking methods (Figs. 6.1–6.2). The rock disaggregation and picking method of foraminiferal species/specimen recovery is the second method that provides a high foraminiferal recovery (Table 2). The microCT scan shows clear resolution for individual well-preserved specimens to visualize the diagnostic inner structures required for accurate identification. However, the resolution in the cutting-bulk (i.e., those in which all the allochems and not only the foraminifera were analyzed with the microCT), was subject to overlapping specimens, foraminiferal test preservation and or x-ray density/contrast similarities between matrix, bioclast, and LBF tests that decreased the efficiency for qualitative/quantitative analyzes. The method is not absolutely perfect, but the results show desirable recovery of microfossil diversity and assemblage context (Tables 1 and 2). This method for the foraminiferal bulks in Eppendorf vials of sorted species/specimens from disaggregated rocks shows excellent scan results (Fig. 8).

The microCT analysis for the highly lithified rock samples has certain limitations in the recovery and recognition of well-preserved

Table 2

Foraminifera. Absolute numbers of species per method (picking, and petrography) from the Pirabas Formation (Miocene), Ilha de Fortaleza (Ponta do Castelo and Fazenda outcrops), Brazilian equatorial platform coastal plain. Data for the empty row (FAZ1-picking) are not available because it was not possible to disaggregate the highly lithified rock using the hot water method.

		FORAMINIFERA (species/specimens number by method)																	Dominant species per methods in %			Counts (n) and relative proportion (%) species/sample/method																
Outcrops	Lithified rock samples by section	Methods *Picking (15g), *Petrography (2)	Ammonia	Amphistegina	Archaias	Cibicides	Cibicidoides	Discorbis	Elphidium	Lagena	Nonioella	Oolina	Pyrgo	Quinqueloculina	Triloculina	Uvigerina	Globigerina	Globigerinella	Globigerinoides	Globobulborotalita	Textularia	Victoriella	SBHyaline	SBPorcelaneous	Amphistegina	Pyrgo	Quinqueloculina	counts all species by method	proportion all species by method									
Ponta do Castelo	PTA1	Picking	1	2	5				1	6				106	7	4	4	1	5	1						1.4	74.1	4.9	143	73.0								
		Petrography		5										4	12							15	4	12	1	9.4	7.5	22.6	53	27.0								
	PTA2	Picking				6								106	42	3										67.5	26.8		157	93.5								
		Petrography		1										4	3								1	2		9.1	36.4	27.3	11	6.5								
	PTA3	Picking	72	343	17	80	2	18	16	1	1	1	1	68	6	1										54.9	10.9	1.0	625	97.7								
		Petrography	4	1										1	2		1						3	3		6.7	13.3		15	2.3								
	PTA4	Picking	6	1	19		22							30	5	3										7.0	34.9	5.8	86	76.8								
Petrography		2											2	4		2						10	1	5	7.7	7.7	15.4	26	23.2									
PTA6	Picking												3												100.0			3	27.3									
	Petrography		1										2	2									3		12.5	25.0	25.0	8	72.7									
PTA7	Picking	8	1			13							26	2											16	52	4.0	50	75.8									
	Petrography	4											1	2								4	5		25.0	6.3	12.5	16	24.2									
Fazenda	FA1	Picking																																				
		Petrography		21										5	16											39.6	9.4	30.2	53	100								
	FA2	Picking	83	8	2		18	3	8					67	24	1	2	1								3.7	30.9	11.1	217	92.35								
		Petrography		1										6	5											5.6	33.3	27.8	18	7.65								
	FA3	Picking		27		1			5					62	11											25.5	58.5	10.4	106	99.1								
		Petrography												1												100.0			1	0.9								
FA5	Picking	2	16	4	4																				61.5			26	39.4									
	Petrography		3										12	12		1						2	10		7.5	30.0	30.0	40	60.6									
FA6	Picking	10	7	6									7									5			28.6	20.0		35	92.1									
	Petrography												1										2		33.3			3	7.9									
Foraminifera recovery (proportion in %) by method			Picking										Mean: 69.73							Petrography										Mean: 30.27								

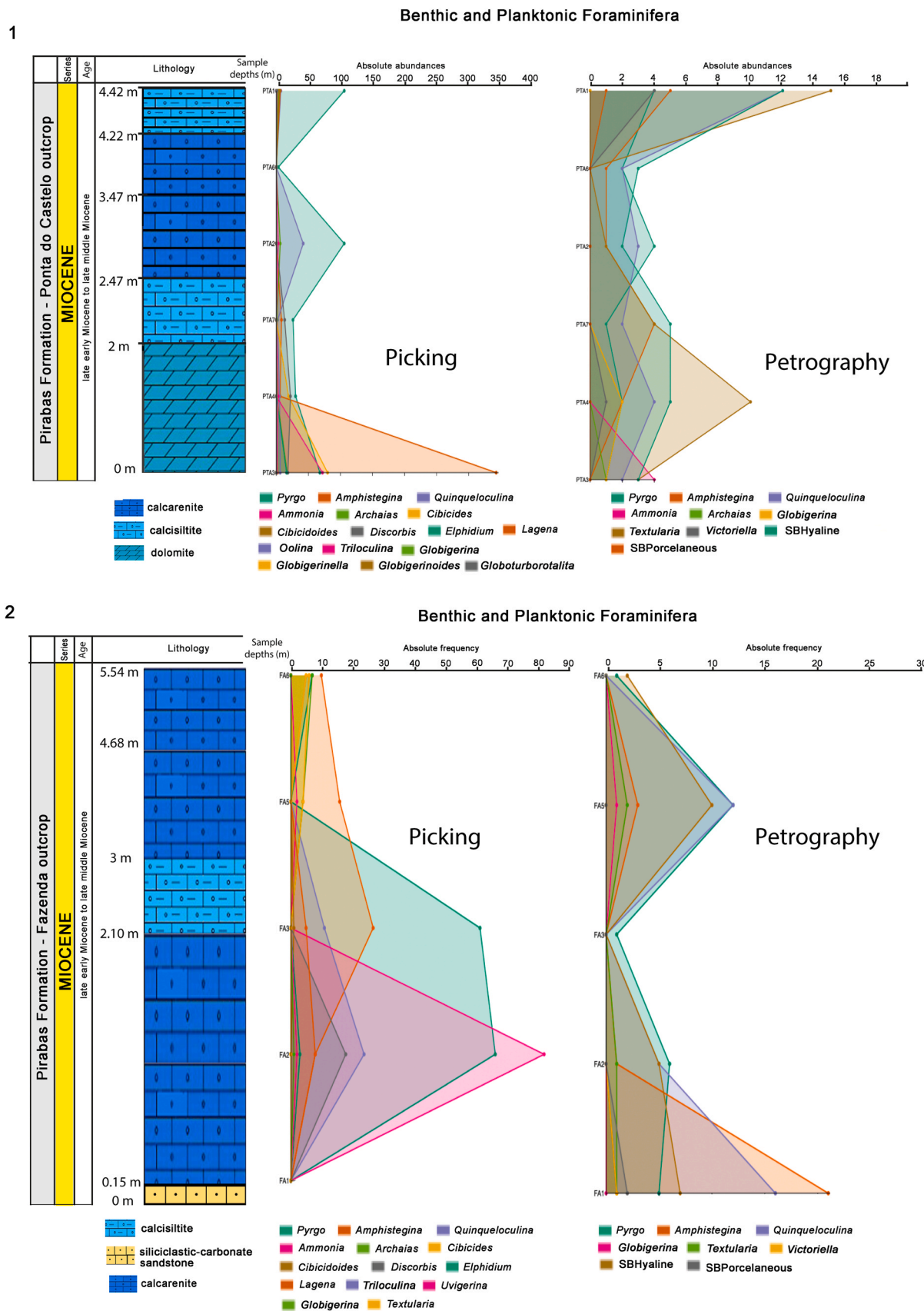


Fig. 5. Benthic and planktonic foraminifera recovered from the Pirabas Formation in the Ilha de Fortaleza outcrops. 1, Ponta do Castelo and 2, Fazenda, using picking and petrography methods. Absolute abundance expressed as stacked areas. The sections follow Teixeira et al. (2024).

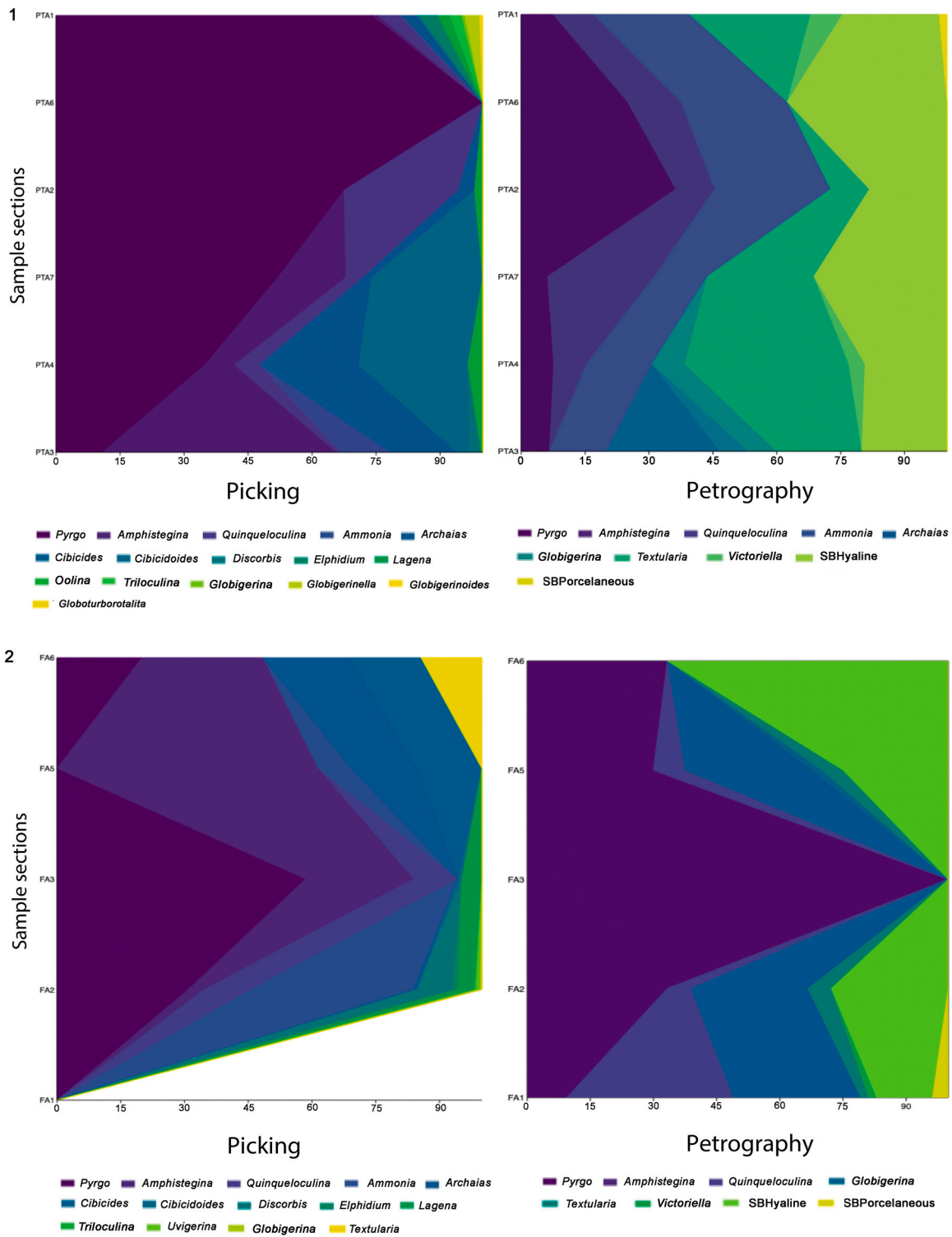
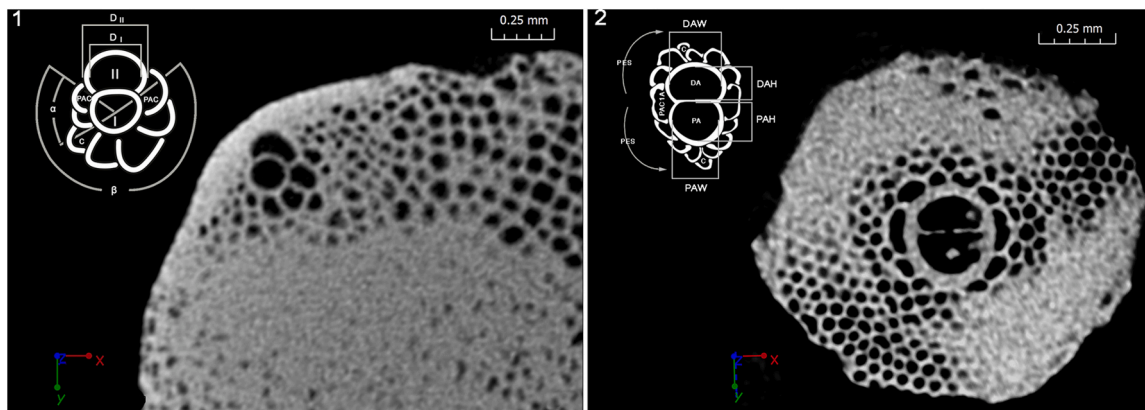


Fig. 6. Benthic and planktonic foraminifera recovered from the Ilha de Fortaleza outcrops. 1, Ponta do Castelo and 2, Fazenda, using picking and petrography methods. Relative abundance expressed as stacked areas.

microfossils (Fig. 9). False impressions of foraminifera diversity and abundance in lithified rocks samples may also result from diagenetic processes. The effectiveness of microCT is lower, particularly for species with extremely similar external morphologies. In contrast, the traditional method, although slower in diagnostic character identification and taxonomic classification, offers more accuracy (Table 3). The microCT method, on the other hand, excels in speed in these aspects.

### 5. Discussion

The comparison of the efficiency and accuracy of the micropaleontology research methods applied herein, including stereomicroscopy, petrographic microscopy, scanning electronic microscopy, and computer digital tomography, suggests that the microCT approach represents the most accurate and efficient method for both industrial and academic micropaleontological research (Figs. 2–6).



**Fig. 7.** MicroCT and schematic drawings of the embryonic apparatus indicating the main biometric parameters and 2D sections of the 3D models of: 1, *Miogypsina* and 2, *Lepidocyclina* from the Ilha de Santana Formation (well 1-MAS-16-MA), Pará-Maranhão Basin, Brazil. Abbreviations: I = protoconch; II deutoconch;  $\alpha$  = angle of shortest spiral around the protoconch;  $\beta$  = angle of both spirals around protoconch; c = closing chambers; DI = diameter of protoconch; DII = diameter of deutoconch; DA = internal area of deutoconch; DAH = height of the DA excluding wall thickness; DAW = width of the DA excluding wall thickness; PA = internal area of protoconch; PAC = primary auxiliary chamber; PAC1A = internal area of the largest auxiliary chamber; PAC2A = internal area of the smallest auxiliary chamber; PAH = height of the PA excluding wall thickness; PAW = width of the PA excluding wall thickness; POS = Periembrionic spire.

**Table 3**

Method procedures and time estimated for each step. However, caution for processing times for individual samples interpretation is necessary, because it is well known that samples processing involve a simultaneous set of samples processing that could be overlapping in time and analyzes (e.g., scanning electron microscope by set of stubs, heating plates or mesh batteries for washing in current water).

CUTTINGS SAMPLES		Time per method	Total
<b>Picking</b>	Subsample pretreatment (acid acetic 5 min, washing 5 min, sieving 5 min, and drying 1 h)	1 h 15 min	
	Picking (all microfossil in the sample)	4 h	
	foraminifera Identification, counts, and catalog	4 h	
	Digital stereomicroscope captions and editions of images (diagnostic well preserved microfossil from the sample)	8 h	
	Edition of database and specimens arrangement in the collections	4 h	21h15min h by subsample
	Pretreatment of specimens (ultrasonic cleaning, metalized and mounting on stub).	1 h	
	Selection of images obtained and recording on digital files	1 h	2 h by stub
	Specimen plug mounting	15 minutes	
	microCT acquisition	30 minutes	
	3D reconstruction, 3D volumetric editing, digital imaging, selection, counts and recording	4 h	4 h 45 min by specimen
<b>Scanning Electron Microscope</b>	Eppendorf vials cuttings sample acquisition	30 minutes	
	LBF biometric assessments, measurements, identification, database, statistical approach	4 h	4 h 30 min by Eppendorf vial content analysis
<b>Petrography</b>	Acrylic block preparation and time for consolidation	24 h	
	Glass slide mounting and polishing	2 h	
	Analyzes, counts, and digital imaging employing a petrographic microscope	1 h	27 h by thin petrographic sectioning
LITHIFIED ROCK		Time per method	Total
<b>Picking</b>	Sample pretreatment by 1 kg rock (boiling water 72 h, sieving 30 min, and drying 4 h)	76 h 30 min	
	Picking 500 $\mu$ m, 250 $\mu$ m, 120 $\mu$ m (1Kg rock sample)	72 h	
	Identification and counts (all microfossils included)	8 h	
	Database and collection	1 h	157 h 30 min by 1 Kg sample from a set of 500, 250, 125 $\mu$ m all microfossils included
<b>Scanning Electron Microscope</b>	Pretreatment of specimens (ultrasonic cleaning, metalizing, and mounting on stub), selection of image records, and recording on digital files	2 h	2 h by stub
<b>Petrography</b>	Obtaining a 3 cm $\times$ 3 cm subsample cut	20 minutes	
	Glass slide mounting and polishing	2 h	
	Analyzes, counts, and digital imaging employing a petrographic microscope	1 h	3 h 20 min by thin petrographic sectioning
<b>MicroCT</b>	Rock block acquisition	45 minutes	
	3D reconstructions, 3D volumetry editing, digital imaging, selection, counts, and recording	4 h	4 h 45 min by block

In this sense, if cutting samples and lithified rock samples contain well-preserved foraminifera, the chances of specimen recovery increases. However, the visualization of diagnostic inner structures for accurate identification using the microCT methods is faster than the manual preparation of thin sections.

Despite the relatively recent advances in microCT concerning foraminifera (Görög et al., 2011; Briguglio et al., 2014, 2016; Ferrández-Cañadell et al., 2014; Renema and Cotton, 2015; Coletti et al., 2018; Aguilera et al., 2020 a, b; Carvalho et al., 2020; Mouro et al., 2021; Alvarado et al., 2023), this method allows for the development of digital

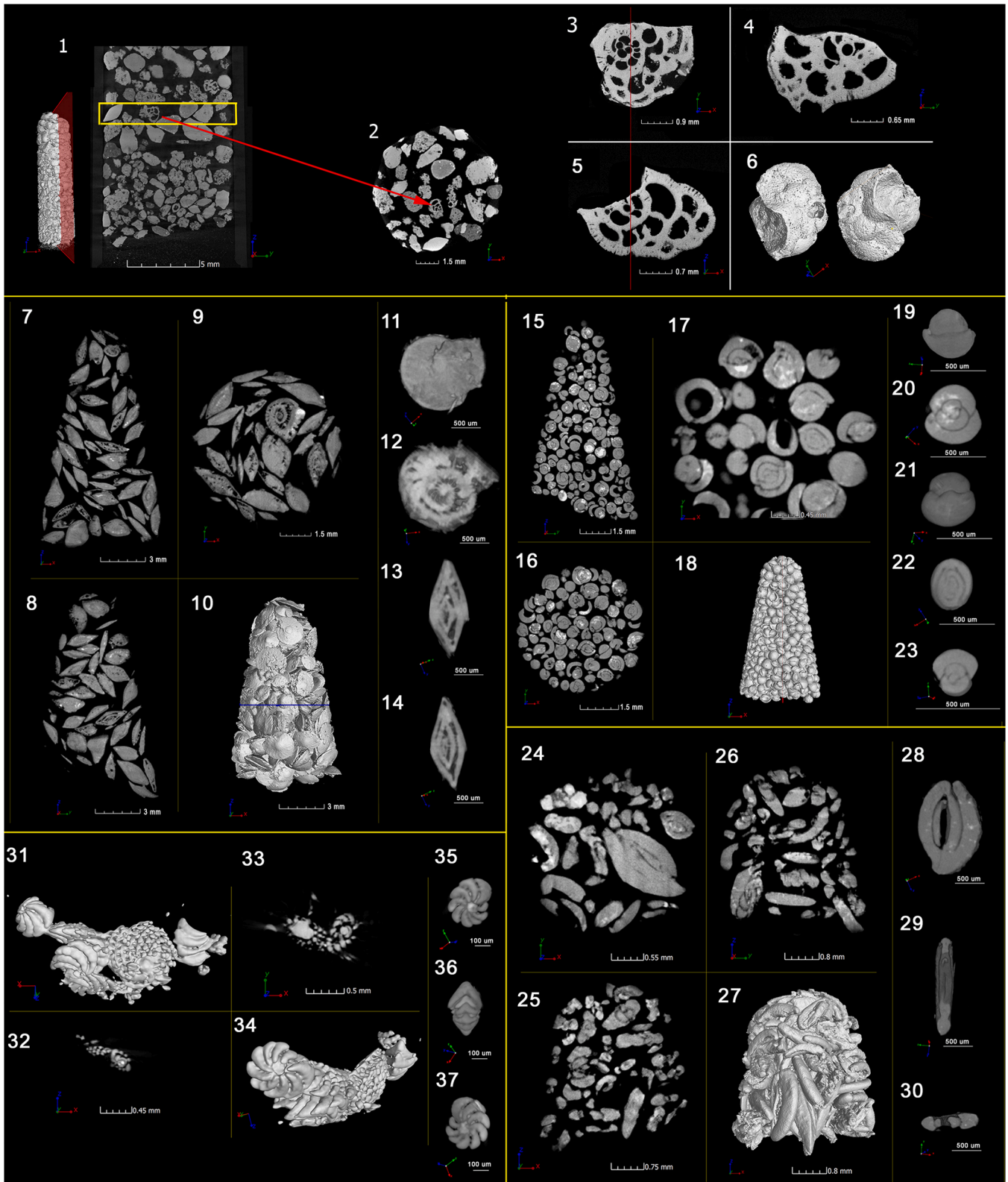


**Fig. 8.** Simplified imagen steps of microCT Eppendorf acquisition from cutting samples from the Ilha de Santa Formation (well 1-MAS-16-MA), equatorial platform of Brazil. 1–6, inner sections and 3D volume of *Victoriella* in rotate views. 7–14, inner sections and 3D volume of *Amphistegina lessonii* recovery from lithified rock from the Pirabas Formation. 15–23, inner sections and 3D volume of *Pyrgo subsphaerica* recovery from lithified rock from the Pirabas Formation. 24–30, inner sections and 3D volume of *Quinqueloculina* recovery from lithified rock from the Pirabas Formation. 31–37, in inner planes views and 3D volume of *Archaia angulatus* recovery from lithified rock from the Pirabas Formation.

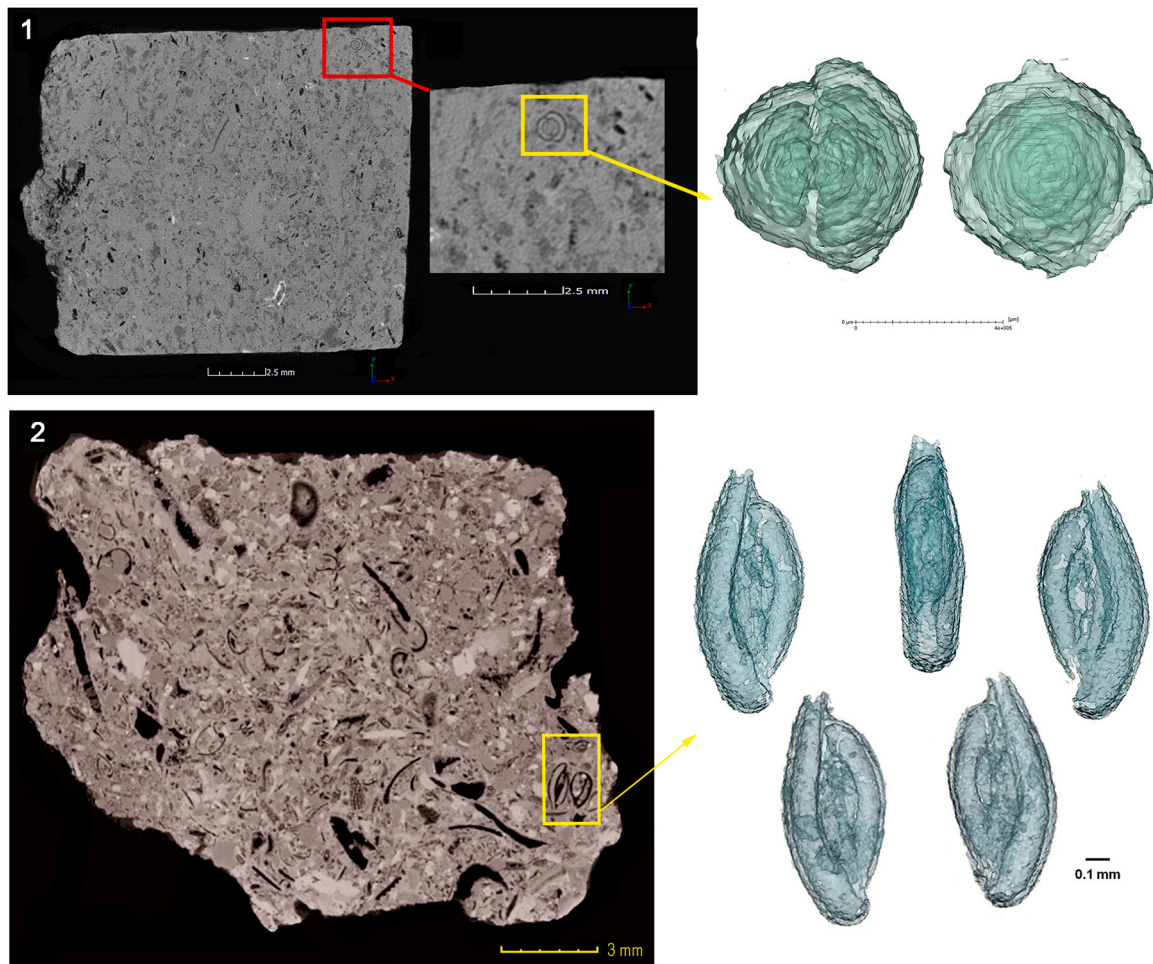


**Fig. 9.** Simplified steps for rock microCT acquisition and foraminifera volumetry. 1, mixed massif siliciclastic-carbonate sandstone sample from the Fazenda outcrop at Ilha de Fortaleza, Brazil, Pirabas Formation (Burdigalian), and *Pyrgo* 3D reconstruction details in rotated views; 2, packstone rock from the Atalaia outcrop at Praia do Atalaia, Brazil, Pirabas Formation, and *Spiroloculina* 3D reconstruction in rotated view.

data useful for accurate taxonomic identification and new artificial intelligence research proposals (Hsiang et al., 2019, 2022; Carvalho et al., 2020; Marchant et al., 2020), creating a wide digital neural network linking microfossil repositories to industrial reservoir exploration settings.

Digitalized rock plug samples (S1\_Video. Packstone), cutting samples (S2\_Video.Eppendorf), and individual LBF specimens (e.g., S3\_Video. *Lepidocyclina*, S4\_Video. *Miogypsina*, and S5\_Video. *Sphaerogypsina*) indicate the irrefutable advantage of microCT analyzes for 3D reconstructions of LBF external morphology and detailed inner sections and structures for accurate taxonomic assessments. However, this method is still expensive due to specialized equipment and software, as well as the need for specialized expertise in associated software. These investments are justified by the quality and speed of results in multi-user laboratories and on an industrial scale.

Supplementary material related to this article can be found online at [doi:10.1016/j.micron.2024.103611](https://doi.org/10.1016/j.micron.2024.103611).

The proposal of this microCT scan method and the comparison with classical methods provides an alternative for acquisition and edition tools to develop a digital foraminiferal species database for taxonomic research and as a baseline for a foraminiferal research machine learning network.

Regardless of the micropaleontological method applied, digitizing collections is the best way to prevent fossil fragmentation during manipulation and allows researchers and students worldwide to easily access the specimens. Some microCT scan limitations are noted, such as

difficulty recognizing foraminiferal specimens embedded in lithified matrices with densities similar to those of the embedding rock matrix, resulting in poor 3D images. Furthermore, smaller foraminifera (50  $\mu\text{m}$  or less) are challenging for high-quality acquisition, and specimen overlaps and agglomerations demand extra time for accurate individual 3D volumetric records. In addition, highly lithified carbonate rock and diagenesis processes may also mask potential microfossil contents.

Other methods investigated herein also display several limitations. For example, random thin rock sections used in petrographical analyzes usually present low probabilities of matching the equatorial LBF plane enough to identify specimens at the species levels, and a large numbers of thin petrographic sections must be manually prepared, specifically searching for the diagnostic equatorial plane in previously isolated LBF specimens. Regarding the stereomicroscope method, external LBF morphology is insufficient for accurate species identification, and lithified rock pretreatment and manual LBF picking, identification, separation, counting and digitalizing are very time-consuming.

In the case of Miocene lithified rocks, the best and most economical method is rock disaggregation and picking, as the taxonomy of Miocene groups (mostly amphisteginids, small benthic and planktonic foraminifera) does not require the search for internal diagnostic structures. However, for cutting samples (core sections) older than the early Miocene and throughout the Paleogene/Cretaceous, the LBF miogypsinids and lepidocyclinids are usefully for age determination/biozones. Therefore, their accurate identification depends on the recognizing the inner diagnostic structures.

Finally, for petrographic analysis, thin sections are required for lithology and paleoenvironment interpretation.

## 6. Conclusions

The comparative analysis of various micropaleontological methods applied to the recovery, identification, and quantification of foraminifera in both cutting and lithified rock samples reveals significant insights. The results demonstrate that microCT emerges as the most accurate and efficient method, offering advantages in terms of speed, accuracy in species identification, and potential for 3D reconstructions. Despite being a relatively recent advancement in foraminiferal research, microCT proves to be highly valuable for creating digital data essential for taxonomic identification and supporting future artificial intelligence research initiatives.

The findings highlight the effectiveness of microCT in recovering a diverse range of taxa, including both index and non-index species. Notably, the method's ability to visualize diagnostic inner structures surpasses traditional techniques, such as stereomicroscopy and petrographic microscopy, leading to faster and more accurate taxonomic classifications.

While acknowledging the associated costs and the need for specialized expertise, the benefits of microCT, especially in multi-user laboratories and industrial settings, justify the investments. The proposed microCT scan method not only contributes to the development of a comprehensive digital foraminiferal species database but also lays the groundwork for potential machine learning networks in foraminiferal research.

Nevertheless, it is crucial to recognize the limitations of each method, such as microCT's challenges in dealing with overlapping specimens and density/contrast similarities between matrix, bioclasts, and foraminifera tests. Additionally, highly lithified rock samples may pose difficulties in recognizing well-preserved microfossils, and smaller foraminifera may present challenges in high-quality acquisition.

Finally, the study advocates for the digitization of collections, regardless of the applied micropaleontological method, to prevent fossil fragmentation and enhance global accessibility to specimens. By addressing the strengths and limitations of each method, the research provides valuable insights for researchers and students engaged in foraminiferal studies, paving the way for further advancements in the field.

## CRedit authorship contribution statement

**Oliveira De Araújo Olga:** Writing – review & editing, Writing – original draft, Methodology, Formal analysis, Data curation, Conceptualization. **Aguilera Orangel:** Writing – review & editing, Writing – original draft, Project administration, Methodology, Investigation, Funding acquisition, Formal analysis, Data curation, Conceptualization. **Alvarado Sierra Dayana:** Writing – review & editing, Methodology, Investigation. **Teixeira Guimarães Beatriz:** Writing – review & editing, Methodology, Investigation, Data curation. **Kutter Vinicius:** Writing – review & editing, Visualization, Validation, Investigation. **Linhares Ana Paula:** Writing – review & editing, Validation, Methodology, Investigation, Formal analysis, Data curation. **Lima Daniel:** Writing – review & editing, Methodology, Formal analysis, Data curation. **Dos Santos Silva Julianny:** Writing – review & editing, Methodology, Data curation. **Lopes Ricardo Tadeu:** Writing – review & editing, Visualization, Validation, Supervision, Project administration, Investigation, Conceptualization.

## Declaration of Competing Interest

The authors declare that the research was conducted in the absence of any commercial or financial relationships that could be construed as a potential conflict of interest.

## Data availability

No data was used for the research described in the article.

## Acknowledgments

This research was funded by the Conselho Nacional de Pesquisa do Brasil - (CNPq 304693/2021–9 to Orangel Aguilera; INCT-ANAIS 406303/2022–3 and 314225/2021 to Ricardo Lopes), Fundação de Amparo à Pesquisa do Estado do Rio de Janeiro (FAPERJ E-26/201.035/2021 to Orangel Aguilera), Coordenação de Aperfeiçoamento de Pessoal de Nível Superior, (CAPES 88887.476179/2020–00 to Olga de Araújo), and Fundação Cearense de Apoio ao Desenvolvimento Científico e Tecnológico (FUNCAP #PV1–0187–00019.01.00/21 and #BP5–0197–00056.01.00/22 to Daniel Lima). The authors would like to thank the National Agency of Petroleum (ANP) and PETROBRAS, Brazil; We thank Maria Virginia Antunes, Hilton Costi, Joelma Lobos, and Isadora Mello for valuable assistance. Thanks to Christiano Ng and Giovanni Colletti for reviewing an earlier version of the manuscript. Thanks, are also to Roberto Romani (Associate Editor of MICRON), and anonymous reviewers for their valuable comments and efforts towards that greatly contributed to improve the present manuscript.

## Supplementary materials

- S1\_Video. Packstone mini-plugs, outcrop sections.
- S2\_Video. Eppendorf with LBF from cutting samples, section at 768 m.
- S3\_Video. *Lepidocyclina* 3D reconstruction, section at 816 m.
- S4\_Video. *Miogypsina* 3D reconstruction, sections at 660 m.
- S5\_Video. *Sphaerogypsina* 3D reconstruction, section at 558 m.

## References

- Abreu, W.S., Regali, M.P.S., Shimabukuro, S., 1986. O Terciário da plataforma continental do Maranhão e Pará, Brasil: Bioestratigrafia e evolução paleoambiental. : An. do XXXIV Congr. Bras. De. Geol., Goiânia 1, 145–159.
- Aguilera, O., Oliveira de Araújo, O.M., Hendy, A., Nogueira, A.A.E., Nogueira, A.C.R., Maurity, C.W., Kutterd, V.T., Martins, M.V.A., Coletti, G., Borba, B., Silva-Caminha, S.A.F., Jaramillo, C., Bencomo, K., Lopes, R.T., 2020a. Palaeontological framework from Pirabas formation (North Brazil) used as potential model for equatorial carbonate platform. J. Mar. Micropaleontol. 154, e101813 <https://doi.org/10.1016/j.marmicro.2019.101813>.
- Aguilera, O., Bencomo, K., Oliveira de Araújo, O.M., Dias, B.B., Coletti, G., Lima, D., Silva-Caminha, S.A.F., Polck, M., Martins, M.V.A., Jaramillo, C., Kutter, V.T., Lopes, R.T., 2020b. Miocene heterozoan carbonate systems from the western Atlantic equatorial margin in South America: the Pirabas Formation. Sediment. Geol. 407, 1–28. <https://doi.org/10.1016/j.sedgeo.2020.105739>.
- Aguilera, O., Martins, M.V.M., Linhares, A.P., Kütter, V.T., Coletti, G., 2022. Palaeoenvironment of the Miocene Pirabas formation mixed carbonate–siliciclastic deposits, Northern Brazil: insights from skeletal assemblages. Mar. Pet. Geol. 145, e105588 <https://doi.org/10.1016/j.marpetgeo.2022.105885>.
- Aguilera, O., Oliveira de Araújo, O.M., Lopes, R.T., Cohen, M., Alvarado, D.S., Guimarães, B.T., Linhares, A.P., Rodriguez, F., Moreira, M., Díaz, R., Gama Filho, H. S., Dos Anjos, M.J., Lima, D., Silva, J.S., Giraud-López, M.J., Kütter, V.T., 2023. Miocene tropical storms: carbonate framework approaches and geochemistry proxies in a reservoir model. Mar. Pet. Geol. 154, e106333 <https://doi.org/10.1016/j.marpetgeo.2023.106333>.
- Al-Awwad, S.F., Collins, L.B., 2013. Arabian carbonate reservoirs: a depositional model of the Arab-D reservoir in Khurais field, Saudi Arabia. AAPG Bull. 97 (7), 1099–1119. <https://doi.org/10.1306/11051212103>.
- Albert-Villanueva, E., Ferrández-Cañadell, C., Bover-Arnal, T., Salas, R., 2017. Larger foraminifera biostratigraphy of the early miocene carbonate platforms of the Falcón Basin. Int. Meet. Sedimentol.
- Alvarado, D.S., Aguilera, O., de Araújo, O.M.O., Lopes, R.T., Gerales, M., Martins, M.V. A., Coletti, G., Guimarães, B.T., Linhares, A.P., Kütter, V.T., 2023. Cenozoic biostratigraphy of larger foraminifera from Equatorial carbonate platform of Northwestern Brazil. Mar. Pet. Geol. 156, e106458 <https://doi.org/10.1016/j.marpetgeo.2023.106458>.
- Amirshankarami, M., Vaziri-Moghaddam, H., Taheri, A., 2007. Sedimentary facies and sequence stratigraphy of the Asmari formation at Chaman-Bolbol, Zagros Basin, Iran. Asian J. Earth Sci. 29, 947–959.
- Benedetti, A., Less, G., Parente, M., Pignatti, J., Cahuzac, B., Torres-Silva, A.I., Buhl, D., 2017. *Heterostegina matteuccii* sp. nov. (Foraminifera: Nummulitidae) from the lower Oligocene of Sicily and Aquitaine: a possible transatlantic immigrant. J. Syst. Palaeontol. 16 (2), 87–110. <https://doi.org/10.1080/14772019.2016.1272009>.

- BouDagher-Fadel, M.K., 2018. Evolution and Geological Significance of Larger Benthic Foraminifera, Second edition. London, UCL Press. <https://doi.org/10.14324/111.9781911576938>.
- BouDagher-Fadel, M.K., Price, G.D., 2010a. American Miogypsinidae: an analysis of their phylogeny and biostratigraphy. *Micropaleontology* 56 (6), 567–586. <https://doi.org/10.2307/40983741>.
- BouDagher-Fadel, M.K., Price, G.D., 2010b. Evolution and paleogeographic distribution of the lepidocyclinids. *J. Foraminif. Res.* 40 (1), 70–108. <https://doi.org/10.2113/gsjfr.40.1.79>.
- BouDagher-Fadel, M.K., Price, G.D., Koutsoukos, E.A.M., 2010. Foraminiferal biostratigraphy and paleoenvironments of the Oligocene-Miocene carbonate succession in Campos Basin, southeastern Brazil. *Stratigraphy* 7 (4), 283–299.
- Brandano, M., Frezza, V., Tomassetti, L., Cuffaro, M., 2009. Heterozoan carbonate in oligotrophic tropical waters: the Attard member of the lower coralliine formation (Upper Oligocene, Malta). *Palaeogeogr. Palaeoclimatol. Palaeoecol.* 274, 54–63. <https://doi.org/10.1016/j.palaeo.2008.12.018>.
- Brandão, J.A.S.L., Feijó, F.J., 1994. Bacia do Foz do Amazonas. *Bol. De. Geociências Petrobras* 8 (1), 91–100.
- Briguglio, A., Woger, J., Wolfgring, E., Hohenegger, J., 2014. Changing investigation perspectives: methods and applications of computer tomography on larger benthic foraminifera. *Approaches Study Living Foraminifera Collect. Maint. Exp.* 55–70. <https://doi.org/10.1007/978-4-431-54388-6>.
- Briguglio, A., Kinoshita, S., Wolfgring, E., Hohenegger, J., 2016. Morphological variations in cycloclypeus carpenteri: multiple embryos and multiple equatorial layers. *Palaeontol. Electron.* 19 (1), 1–22, 3A.
- Bruhn, C.H.L., Gomes, J.A.T., Del Lucchese, Jr.C., Johann, P.R.S., 2003. Campos Basin: reservoir characterization and management – historical overview and future challenges. *Offsh. Technol. Conf. OTC 15220*. <https://doi.org/10.4043/15220-MS>.
- Carvalho, L.E., Fauth, G., Baecker Fauth, S., Krahl, G., Moreira, A.C., Fernandes, C.P., von Wangenheim, A., 2020. Automated microfossil identification and segmentation using a deep learning approach. *Mar. Micropaleontol.* 158, e101890 <https://doi.org/10.1016/j.marmicro.2020.101890>.
- Castillo, V., Benkovics, L., Cobos, C., Demuro, D., Franco, A., 2017. Perla field: the largest discovery ever in Latin America. In: Merrill, R., Sternbach, C. (Eds.), *Memoir 113: Giant Fields of the Decade 2000–2010*. AAPG, pp. 141–152.
- Chaproniere, G.C.H., 1980. Biometrical studies of early neogene larger foraminifera from Australia and New Zealand. *Alcheringa* 4, 153–181.
- Coletti, G., Basso, D., Frixia, A., 2017. Economic importance of coralline carbonates, Rhodolith/Maërl Beds: A Global Perspective. *Coastal Research Library*, 15. Springer Cham, pp. 87–101, 10.1007/978-3-319-29315-8\_4.
- Coletti, G., Stainbank, S., Fabbrini, A., Spezzaferri, S., Foubert, A., Kroon, D., Betzler, C., 2018. Biostratigraphy of large benthic foraminifera from Hole U1468A (Maldives): a CT-scan taxonomic approach. *Swiss J. Geosci.* 111, 523–536. <https://doi.org/10.1007/s00015-018-0306-7>.
- Cotton, L.J., Eder, W., Floyd, J., 2018. Larger foraminifera of the Devils Den and Blue Hole sinkholes, Florida. *J. Micropaleontol.* 37, 347–356. <https://doi.org/10.5194/jm-37-347-2018>.
- Ferrández-Cañadell, C., Briguglio, A., Hohenegger, J., Wöger, J., 2014. Test fusion in adult foraminifera: a review with new observations of an early Eocene nummulites specimen. *Eur. PMC Funders Group* 44 (3), 316–324. <https://doi.org/10.2113/gsjfr.44.3.316>.
- Figueiredo, J., Zalán, P.V., Soares, E.F., 2007. Bacia da Foz do Amazonas. *Bol. De. Geociências Petrobras* 15, 299–309.
- Fiorini, F., Jaramillo, C., 2007. Paleoenvironmental reconstruction of the Oligocene-Miocene deposits of Southern Caribbean (Carmen de Bolívar, Colombia) based on benthic foraminifera, 329–329 *Anu.ário do Inst. De. Geociências* 29 (1). [https://doi.org/10.11137/2006\\_1\\_329-329](https://doi.org/10.11137/2006_1_329-329).
- François, D., Paytan, A., de Araújo, O.M.O., Lopes, R.T., Barbosa, C.F., 2022. Acidification impacts and acclimation potential of Caribbean benthic foraminifera assemblages in naturally discharging low-pH water. *Biogeosciences* 19, 5269–5285. <https://doi.org/10.5194/bg-19-5269-2022>.
- Ghafor, I.M., 2014. Biometric analysis of *Lepidocyclusina* (*Nephrolepidina*) from Baba Formation (Late Oligocene) in Bai-Hassan Well-25, Kirkuk Area, Northeast Iraq. *Sci. Res.* 2 (5), 111–118. <https://doi.org/10.11648/j.sr.20140205.16>.
- Gomes, B.T., Aguilera, O., Silva-Caminha, S.A.F., D'Apollito, C., Cárdenas, D., Hocking, E. P., Lemes, K.K.B., 2023. Biostratigraphy and Paleoenvironments of the Pirabas Formation (Neogene, Pará State-Brazil). *Mar. Micropaleontol.* 180, 102218 <https://doi.org/10.1016/j.marmicro.2023.102218>.
- Görög, Á., Szinger, B., Tóth, E., Viskok, J., 2011. Methodology of the micro-computer tomography in foraminifera. *Palaeontol. Electron.* 15 (1), 15p, 3T.
- Green, O.R., 2001. A manual of practical laboratory and field techniques in palaeobiology: washing and sieving techniques used in micropaleontology, 16. Springer, pp. 146–153, 10.1007/978-94-017-0581-3\_16.
- Hohenegger, J., Torres-Silva, A.L., 2020. Methods for testing ontogenetic changes of neanic chamberlets in Lepidocyclinids. *J. Foraminif. Res.* 50 (2), 182–194. <https://doi.org/10.2113/gsjfr.50.2.182>.
- Hsiang, A.Y., Hull, P.M., 2022. Automated community ecology using deep learning: a case study of planktonic foraminifera. *BioRxiv*. <https://doi.org/10.1101/2022.10.31.514514>.
- Hsiang, A.Y., Brombacher, A., Rillo, M.C., Mleneck-Vautravers, M.J., Conn, S., Lordsmith, S., Jentzen, A., Henehan, M.J., Metcalfe, B., Fenton, I.S., Wade, B.S., Fox, L., Meilland, J., Davis, C.V., Baranowski, U., Groeneveld, J., Edgar, K.M., Movellan, A., Aze, T., Dowsett, H.J., Miller, C.G., Rios, N., Hull, P.M., 2019. Endless Forams: >34,000 modern planktonic foraminiferal images for taxonomic training and automated species recognition using convolutional neural networks. *Paleoceanogr. Paleoclimatol.* 34, 1157–1177 <https://doi.org/10.1029/2019PA003612>.
- Khodja, M.R., Li, J., Hussaini, S.R., Ali, A.Z., Al-Mukainah, H.S., Jangda, Z.Z., 2020. Consistent prediction of absolute permeability in carbonates without upscaling. *Oil Gas. Sci. Technol. Rev. D. IFP Energ. Nouv.* 75, 44. <https://doi.org/10.2516/ogst/2020029>.
- Less, G., Özcan, E., Papazzoni, C.A., Stockar, R., 2008. The middle to late eocene evolution of nummulitid foraminifer *Heterostegina* in the Western Tethys. *Acta Palaeontol. Pol.* 53, 317–350.
- Mahmoodabadi, R.M., Zahiri, S., 2022. Formation evaluation and rock type classification of Asmari Formation based on petrophysical- petrographic data: a case study in one of super fields in Iran southwest. *Petroleum*. <https://doi.org/10.1016/j.petlm.2022.01.009>.
- Malik, M.H., Chan, S.A., Babalola, L.O., Kaminski, M.A., 2022. Optimization of the acetic acid method for microfossil extraction from lithified carbonate rocks: examples from the Jurassic and Miocene limestones of Saudi Arabia. *MethodsX* 9, e101828. <https://doi.org/10.1016/j.mex.2022.101828>.
- Marchant, R., Tetard, M., Pratiwi, A., de Garidel-Thoron, T., 2020. Automated analysis of foraminifera fossil records by image classification using a convolutional neural network. *J. Micropaleontol.* 39 (2), 183–202. <https://doi.org/10.5194/jm-39-183-2020>.
- Matteucci, R., Schiavinotto, F., 1977. Studio biometrico di Nephrolepidina, Eulepidina e Cycloclypeus in due campioni dell'Oligocene di Monte La Rocca, LAquila (Italia centrale). *Geol. Romana* 16, 141–171.
- Maury, C.J., 1925. Fósseis terciários do Brasil com descrição de novas formas Cretáceas. *Serviço Geol. ógico e Miner. ógico do Bras., Monogr.* 4, 665 p.
- de Mello e Sousa, S.H., Rossetti, D., Fairchild, T.R., Buron, L., de Mahiques, M.M., Tibana, P., 2009. Microfacies and sequence stratigraphy of the Amapá Formation, Late Paleocene to Early Eocene, Foz do Amazonas Basin, Brazil. *Palaeogeogr., Palaeoclimatol. Palaeoecol.* 280, 440–455. <https://doi.org/10.1016/j.palaeo.2009.06.031>.
- de Mello e Sousa, S.H., 1994. Estudo microfossilológico da Formação Amapá (Terciário), Bacia da Foz do Amazonas: interpretações bioestratigráficas e paleoecológicas. Tese Doutorado. Inst. Geociência. USP.
- de Mello e Souza, S.H., Fairchild, T.R., TibanaP., 2003. Cenozoic biostratigraphy of larger foraminifera from the Foz do Amazonas Basin, Brazil. *Micropaleontology* 49 (3), 253–266. 10.1661/00262803(2003)049[0253:CBOLFF]2.0.CO;2.
- Mitchell, S.F., Robinson, E., Özcan, E., Jiang, M.M., Robinson, N., 2022. A larger benthic foraminiferal zonation for the Eocene of the Caribbean and central American region. *Carnets De. Geol.* 22 (11), 409–565.
- Mouro, L.D., Vieira, L.D., Moreira, A.C., Piovesan, E.K., Fernandes, C.P., Fauth, G., Horodisky, R.S., Ghilardi, R.P., Mantovani, I.F., Backer-Fauh, S., Krahl, G., Waichel, B.L., da Silva, M.S., 2021. Testing the X-ray computed microtomography on microfossil identification: an example from Sergipe-Alagoas Basin, Brazil. *J. South Am. Earth Sci.* 107, e103074 <https://doi.org/10.1016/j.jsames.2020.103074>.
- Muhammed, Q.A., Ghafor, I.M., 2008. Biometric analysis of miogypsinidae and their taxonomic significance from Azkand formation (Oligocene-Miocene) in Kirkuk area, Iraq. *Tikrit J. Pure Sci.* 13 (1), 198–213.
- Özcan, E., Less, G., Baldi-Beke, M., Kollányi, K., Acar, F., 2009. Oligo-Miocene foraminiferal record (Miogypsinidae, Lepidocyclinidae and Nummulitidae) from the Western Taurides (SW Turkey): biometry and implications for the regional geology. *J. Asian Earth Sci.* 34, 740–760.
- Özcan, E., Mitchell, S.F., Less, G., Robinson, E., Bryan, J.R., Pignatti, J., Yücel, A.O., 2019. A revised suprageneric classification of American orthophragminids with emphasis on late Paleocene representatives from Jamaica and Alabama. *J. Syst. Palaeontol.* 17 (18), 1–29 <https://doi.org/10.1080/14772019.2018.1539778>.
- Pemberton, S.G., Gingras, M.K., 2005. Classification and characterizations of biogenically enhanced permeability. *AAPG Bull.* 89 (11), 1493–1517. <https://doi.org/10.1306/07050504121>.
- Perry, O.R., Choquette, P.W., 1985. Carbonate petroleum reservoirs. Springer, New York. <https://doi.org/10.1007/978-1-4612-5040-1>.
- Pessoa Neto, O. da C., 1999. Análise estratigráfica integrada da plataforma mista (Siliciclástica-Carbonática) do Neogeno da Bacia Potiguar, Nordeste do Brasil. Dissertação de Mestrado, Instituto de Geociências, Universidade Federal do Rio Grande do Sul, Brasil.
- Petri, S., 1954. Foraminíferos fósseis da Bacia do Marajó. *Bol. da Fac. De. Filos., Ciências e Let. da Univ. De. São Paulo. Geol.* (11), 4–144.
- Petri, S., 1957. Foraminíferos Miocênicos da Formação Pirabas. *Bol. da Fac. De. Filos., Ciências e Let. da Univ. De. São Paulo. Geol.* 216, 1–172.
- Renema, W., Cotton, L., 2015. Nummulites tests reveal complex chamber shapes. *PeerJ* 3, e1072. <https://doi.org/10.7717/peerj.1072>.
- Robinson, E., 2003. Zoning the white limestone group of Jamaica using larger foraminiferal genera: a review and proposal. *Cainozoic Res.* 3 (1/2), 39–75.
- Rojas, L.E.G., Nogueira, A.A.E., Soares, J.L., Nogueira, A.C.R., Imbiriba, Jr.M., 2022. Biostratigraphy and paleoenvironment correlation based on benthic foraminifera from the Cenozoic Marajó and Pirabas formations, Eastern Amazon Coast, Brazil. *J. South Am. Earth Sci.* 120 (3), e104035 <https://doi.org/10.1016/j.jsames.2022.104035>.
- Rossetti, D.F., 2006. Evolução sedimentar miocênica nos estados do Pará e Maranhão. *Geol. USP Sêrie Cient. ífica, São Paulo* 6 (2), 7–18. <https://doi.org/10.5327/S1519-874x2006000300003>.
- Rossetti, D.F., Truckenbrodt, W., Góes, A.M., 1989. Estudo paleoambiental e estratigráfico dos sedimentos Barreiras e Pós-Barreiras na região Bragançana, nordeste do Pará. *Boletim do Museu Paraense Emílio Goeldi, Série Ciências da Terra* 1 (1), 25–74.

- Rossetti, D.F., Bezerra, F.H.R., Dominguez, J.M.L., 2013. Late Oligocene–Miocene transgressions along the equatorial and eastern margins of Brazil. *Earth Sci. Rev.* 123, 87–112. <https://doi.org/10.1016/j.earscirev.2013.04.005>.
- Schiavinotto, F., 1978. *Nephrolepidina nella Valle del Maso (Borgo Valsugana - Italia settentrionale)*. *Riv. Ital. di Paleontol. e Stratigr.* 84, 729–750.
- Soares, E.F., Zalán, P.V., Figueiredo, J.-J.P., Trosdorf Jr., I., 2007. Bacia do Pará-Maranhão. *Bol. De. Geociências da Petrobras* 15 (2), 321–329.
- Távora, V., Fernandes, J.M., 1999. Estudio de los foraminíferos de la Formación Pirabas (Mioceno Inferior), estado de Pará, Brasil y su correlación con faunas del Caribe. *Rev. De. Geol. ógica De. Am. érica Cent.* 22, 63–74.
- Teixeira, B.G., Aguilera, O., Linhares, A.P., de Araújo, O.M.O., Mello, I., Costi, H.T., Dayana Alvarado, D.S., Kutter, V., Lima, D., Andrade, G.C.C., Lopes, R., 2024. Paleontological study of the Oligocene/Miocene boundary in the Ilha DE Santana and Pirabas formations, Para-Maranhão basin on the Northwest equatorial platform of Brazil. *J. South Am. Earth Sci.*, 104784 <https://doi.org/10.1016/j.jsames.2024.104784>.
- Torres-Silva, A.I., Hohenegger, J., Coric, S., Briguglio, A., Eder, W., 2017. Biostratigraphy and evolutionary tendencies of Eocene Heterostegines in western and central Cuba based on morphometric analyses. *Palaios* 32 (1), 44–60. <https://doi.org/10.2110/palo.2016.004>.
- Van der Vlerk, I.M., 1959. Modifications de l'ontogénèse pendant l'évolution des Lépidocyclines (Foraminifères). *Bull. De. la Soci. été Géologique De. Fr. Notes Et. Mémoires Série 1* (7), 669–673.
- Van der Vlerk, I.M., 1963. Biometric research on *Lepidocyclina*. *Micropaleontology* 9, 425–426.
- Van Vesseem, E.J., 1978. Study of Lepidocyclinidae from south-east Asia, particularly from Java and Borneo. *Utrecht Micropaleontol. Bull.* 19, 1–163.
- Wong, T., Geuns, L., 2019. The discovery of a major hydrocarbon occurrence in the Guiana Basin, offshore Suriname: a blessing or a curse? *Acad. J. Suriname* 10, 1–6.